DOI: 10.1021/ic102217z

Inorganic Chemistry
Article

Nature of M−Ga Bonds in Cationic Metal-Gallylene Complexes of Iron, Ruthenium, and Osmium, $[(\eta^5\text{-}C_5H_5)(L)_2M(GaX)]^+$: A Theoretical Study

Krishna K. Pandey*,† and Simon Aldridge*,‡

†*School of Chemical Sciences, Devi Ahilya University Indore, Indore 452001, India, and* ‡*Inorganic Chemistry Laboratory, Department of Chemistry, University of Oxford, South Parks Road, Oxford OX1 3QR, U.K.*

Received November 4, 2010

Density Functional Theory calculations have been performed for the cationic half-sandwich gallylene complexes of iron, ruthenium, and osmium $[(\eta^5\text{-}C_5H_5)(L)_2M(GaX)]^+$ (M = Fe, L = CO, PMe_3; X = Cl, Br, I, NMe_2, Mes; M = Ru, Os: L = CO, PMe_3; X = I, NMe_2, Mes) at the BP86/TZ2P/ZORA level of theory. Calculated geometric parameters for the model iron iodogallylene system $[(\eta^5\text{-}C_5H_5)(Me_3P)_2Fe(GaI)]^+$ are in excellent agreement with the recently reported experimental values for $[(\eta^5\text{-}C_5Me_5)(dppe)Fe(GaI)]^+$. The M−Ga bonds in these systems are shorter than expected for single bonds, an observation attributed not to significant M−Ga π orbital contributions, but due instead primarily to high gallium s-orbital contributions to the M−Ga bonding orbitals. Such a finding is in line with the tenets of Bent's Rule insofar as correspondingly greater gallium p-orbital character is found in the bonds to the (more electronegative) gallylene substituent X. Consistent with this, ΔE_σ is found to be overwhelmingly the dominant contribution to the orbital interaction between $[(\eta^5\text{-}C_5H_5)(L)_2M]^+$ and [GaX] fragments (with ΔE_π equating to only 8.0−18.6% of the total orbital contributions); GaX ligands thus behave as predominantly σ-donor ligands. Electrostatic contributions to the overall interaction energy ΔE_{int} are also very important, being comparable in magnitude (or in some cases even larger than) the corresponding orbital interactions.

Introduction

Studies of synthetic methodology, electronic structure, and reactivity relating to transition metal borylene complexes, $L_nM(BX)_m$, have been extensively reported since the first structurally characterized systems were unveiled in 1998.[1−22] By contrast, relatively few two-coordinate ligand systems featuring the heavier Group 13 elements have been investigated to date, and the nature of M−E bonding in such complexes has, at times, ignited fierce debate.[23] Among these systems, a number of transition metal gallylene complexes have been reported (Chart 1), but to date analogous (two-coordinate)

*To whom correspondence should be addressed. E-mail: kkpandey.schem@dauniv.ac.in (K.K.P.), simon.aldridge@chem.ox.ac.uk (S.A.).

(1) Braunschweig, H.; Kollann, C.; Englert, U. *Angew. Chem., Int. Ed.* **1998**, *37*, 3179.
(2) Cowley, A. H.; Lomeli, V.; Voigt, A. *J. Am. Chem. Soc.* **1998**, *120*, 6401.
(3) Braunschweig, H.; Colling, M.; Kollann, C.; Stammler, H. G.; Neumann, B. *Angew. Chem., Int. Ed.* **2001**, *40*, 2298.
(4) Braunschweig, H.; Colling, M.; Kollann, C.; Merz, K.; Radacki, K. *Angew. Chem., Int. Ed.* **2001**, *40*, 4198.
(5) Braunschweig, H.; Colling, M.; Hu, C.; Radacki, K. *Angew. Chem., Int. Ed.* **2003**, *42*, 205.
(6) Braunschweig, H.; Radacki, K.; Rais, D.; Uttinger, K. *Angew. Chem., Int. Ed.* **2006**, *45*, 162.
(7) Braunschweig, H.; Radacki, K.; Rais, D.; Uttinger, K. *Organometallics* **2006**, *25*, 5159.
(8) Blank, B.; Colling-Hendelkens, M.; Kollann, C.; Radacki, K.; Rais, D.; Uttinger, K.; Whittell, G. R.; Braunschweig, H. *Chem.—Eur. J.* **2007**, *13*, 4770.
(9) Braunschweig, H.; Burzler, M.; Kupfer, T.; Radacki, K.; Seeler, F. *Angew. Chem., Int. Ed.* **2007**, *46*, 7785.
(10) Braunschweig, H.; Forster, M.; Kupfer, T.; Seeler, F. *Angew. Chem., Int. Ed.* **2008**, *47*, 5981.
(11) Braunschweig, H.; Kupfer, T.; Radacki, K.; Schneider, A.; Seeler, F.; Uttinger, K.; Wu, H. *J. Am. Chem. Soc.* **2008**, *130*, 7974.
(12) Alcaraz, G.; Helmstedt, U.; Clot, E.; Vendier, L.; Sabo-Etienne, S. *J. Am. Chem. Soc.* **2008**, *130*, 12878.
(13) Coombs, D. L.; Aldridge, S.; Jones, C.; Willock, D. J. *J. Am. Chem. Soc.* **2003**, *125*, 6356.
(14) Coombs, D. L.; Aldridge, S.; Rossin, A.; Jones, C.; Willock, D. J. *Organometallics* **2004**, *23*, 2911.
(15) Aldridge, S.; Jones, C.; Gans-Eichler, T.; Stasch, A.; Kays, D. L.; Coombs, N. D.; Willock, D. J. *Angew. Chem., Int. Ed.* **2006**, *45*, 6118.
(16) Vidovic, D.; Findlater, M.; Reeske, G.; Cowley, A. H. *Chem. Commun.* **2006**, 3786.
(17) Braunschweig, H.; Radacki, K.; Uttinger, K. *Angew. Chem., Int. Ed.* **2007**, *46*, 3979.
(18) Pierce, G. A.; Vidovic, D.; Kays, D. L.; Coombs, N. D.; Thompson, A. L.; Jemmis, E. D.; De, S.; Aldridge, S. *Organometallics* **2009**, *28*, 2947.
(19) De, S.; Pierce, G. A.; Vidovic, D.; Kays, D. L.; Coombs, N. D.; Jemmis, E. D.; Aldridge, S. *Organometallics* **2009**, *28*, 2961.
(20) Addy, D. A.; Pierce, G. A.; Vidovic, D.; Mallick, D.; Jemmis, E. D.; Goicoechea, J. M.; Aldridge, S. *J. Am. Chem. Soc.* **2010**, *132*, 4586.
(21) Braunschweig, H.; Dewhurst, R. D.; Schneider, A. *Chem. Rev.* **2010**, *110*, 3924.
(22) Vidovic, D.; Pierce, G. A.; Aldridge, S. *Chem. Commun.* **2009**, 1157.
(23) (a) Su, J. R.; Li, X.-W.; Crittendon, R. C.; Campana, C. F.; Robinson, G. H. *Organometallics* **1997**, *16*, 4511. (b) Cotton, F. A.; Feng, X. *Organometallics* **1998**, *17*, 128.
(24) Yang, X.-J.; Quillian, B.; Wang, Y. Z.; Wei, P. R.; Robinson, G. H. *Organometallics* **2004**, *23*, 5119.

Published on Web 01/04/2011

Chart 1. Selected Structurally Characterized Two-Coordinate Metal-Gallylene Complexes [Ar = C_6H_3-2,6-$Trip_2$; Trip = 2,4,6-$^iPr_3C_6H_2$]

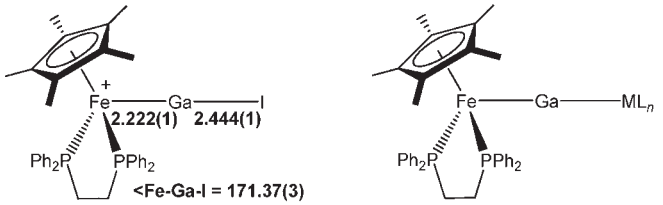

ML_n	*d*(Fe-Ga)	*d*(M-Ga)	<Fe-Ga-M
$Fe(CO)_4$	**2.248(1)**	**2.293(1)**	**176.0(1)**
$Fe(CO)_3PMe_3$	**2.277(1)**	**2.269(1)**	**177.4(1)**
$Fe(CO)_3P(OPh)_3$	**2.269(1)**	**2.285(1)**	**176.4(1)**
$W(CO)_5$	**2.269(1)**	**2.586(1)**	**173.8(1)**

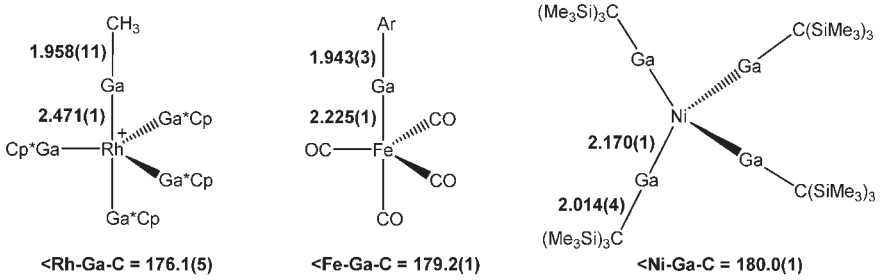

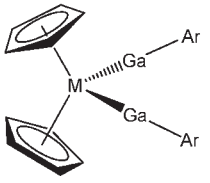

M	*d*(M-Ga)	*d*(Ga-C)	<M-Ga-C
Ti	**2.249(2)**	**2.025(3)**	**171.0(1)**
Zr	**2.635(1)**	**2.003(1)**	**172.4(2)**
Hf	**2.620(1)**	**2.021(1)**	**171.7(3)**

aluminum-containing ligands have thus far eluded experimental study.[23−33] Related transition metal complexes featuring ligands of the types Al(η^5-C_5R_5) and Ga(η^5-C_5R_5) (and which incorporate higher-coordinate Group 13 centers) have, however, been reported.[34−39]

Of particular relevance to the current study are (i) reports of the synthetic, structural and reaction chemistry of [(η^5-C_5Me_5)(dppe)Fe(GaI)]$^+$[BAr^f_4]$^-$, which features a terminally bound GaI ligand, valence isoelectronic with N_2 and CO; and (ii) mass spectrometric studies of the related mesitylgallylene complex [(η^5-C_5Me_5)$(CO)_2$Fe(GaMes)]$^+$, generated by in situ loss of dtbpy from [(η^5-C_5Me_5)$(CO)_2$Fe(GaMes·dtbpy)]$^+$[BAr^f_4]$^-$ [dppe = 1,2-*bis*(diphenylphosphino)ethane, $Ph_2CH_2CH_2PPh_2$; Mes = $C_6H_2Me_3$-2,4,6; Ar^f = $C_6H_3(CF_3)_2$-3,5; dtbpy = 4,4′-di-*tert*-butyl-2,2′-bipyridyl].[31,32]

From a quantum chemical perspective, a number of studies of terminal metal borylene, alylene, and gallylene complexes have been reported, focusing in the main on charge neutral systems related to classical metal carbonyl systems such as $Cr(CO)_6$, $Fe(CO)_5$, and $Ni(CO)_4$.[40−53] To the best of our knowledge, bonding energy analyses of *cationic* half-sandwich complexes of the types [(η^5-C_5H_5)$(L)_n$M(GaX)]$^+$ have not been studied before in depth.[51] Given this deficiency, together with the aforementioned experimental reports of a

(25) Yang, X.-J.; Wang, Y. Z.; Quillian, B.; Wei, P. R.; Chen, Z.; Schleyer, P. v. R.; Robinson, G. H. *Organometallics* **2006**, *25*, 925.
(26) Quillian, P.; Wang, Y.; Wei, P.; Robinson, G. H. *New. J. Chem.* **2008**, *32*, 774.
(27) Uhl, W.; Benter, M.; Melle, S.; Saak, W.; Frenking, G.; Uddin, J. *Organometallics* **1999**, *18*, 3778.
(28) Ueno, K.; Watanabe, T.; Tobita, H.; Ogino, H. *Organometallics* **2003**, *22*, 4375.
(29) Muraoka, T.; Motohashi, H.; Hirotsu, M.; Ueno, K. *Organometallics* **2008**, *27*, 3918.
(30) Muraoka, T.; Motohashi, H.; Kazuie, Y.; Takizawa, A.; Ueno, K. *Organometallics* **2009**, *28*, 1616.
(31) Coombs, N. D.; Clegg, W.; Thompson, A. L.; Willock, D. J.; Aldridge, S. *J. Am. Chem. Soc.* **2008**, *130*, 5449.
(32) Coombs, N. D.; Vidovic, D.; Day, J. K.; Thompson, A. L.; Le Pevelen, D. D.; Stasch, A.; Clegg, W.; Russo, L.; Male, L.; Hursthouse, M. B.; Willock, D. J.; Aldridge, S. *J. Am. Chem. Soc.* **2008**, *130*, 16111.
(33) Cadenbach, T.; Gemel, C.; Zacher, D.; Fischer, R. A. *Angew. Chem., Int. Ed.* **2008**, *47*, 3438.
(34) Weiss, J.; Stetzkamp, D.; Nuber, B.; Fischer, R. A.; Boehme, C.; Frenking, G. *Angew. Chem., Int. Ed.* **1997**, *36*, 70.
(35) Yu, Q.; Purath, A.; Donchev, A.; Schnöckel, H. *J. Organomet. Chem.* **1999**, *584*, 94.
(36) Buchin, B.; Steinke, T.; Gemel, C.; Cadenbach, T.; Fischer, R. A. *Z. Anorg. Allg. Chem.* **2005**, *631*, 2756.
(37) Steinke, T.; Gemel, C.; Winter, M.; Fischer, R. A. *Chem.—Eur. J.* **2005**, *11*, 1636.
(38) Cadenbach, T.; Gemel, C.; Bollermann, T.; Fischer, R. A. *Inorg. Chem.* **2009**, *48*, 5021 and references therein.
(39) Cadenbach, T.; Gemel, C.; Schmid, R.; Halbherr, M.; Yusenko, K.; Cokoja, M.; Fischer, R. A. *Angew. Chem., Int. Ed.* **2009**, *48*, 3872.
(40) Ehlers, A. W.; Baerends, E. J.; Bickelhaupt, F. M.; Radius, U. *Chem.—Eur. J.* **1998**, *4*, 210.
(41) Radius, U.; Bickelhaupt, F. M.; Ehlers, A. W.; Goldberg, N.; Hoffmann, R. *Inorg. Chem.* **1998**, *37*, 1080.
(42) Macdonald, C. L. B.; Cowley, A. H. *J. Am. Chem. Soc.* **1999**, *121*, 12113.
(43) Boehme, C.; Frenking, G. *Chem.—Eur. J.* **1999**, *5*, 2184.
(44) (a) Uddin, J.; Boehme, C.; Frenking, G. *Organometallics* **2000**, *19*, 571. (b) Doerr, M.; Frenking, G. *Z. Anorg. Allg. Chem.* **2002**, *628*, 843.
(45) Chen, Y.; Frenking, G. *Dalton Trans.* **2001**, 434.
(46) (a) Uddin, J.; Frenking, G. *J. Am. Chem. Soc.* **2001**, *123*, 1683. (b) Gámez, J. A.; Tonner, R.; Frenking, G. *Organometallics* **2010**, *29*, 5676.
(47) Bollwein, T.; Brothers, P. J.; Hermann, H. L.; Schwerdtfeger, P. *Organometallics* **2002**, *21*, 5236.
(48) Boehme, C.; Uddin, J.; Frenking, G. *Coord. Chem. Rev.* **2000**, *197*, 249.
(49) Frenking, G.; Fröhlich, N. *Chem. Rev.* **2000**, *100*, 717.
(50) Frenking, G.; Wichmann, K.; Fröhlich, N.; Loschen, C.; Lein, M.; Frunzke, J.; Rayon, V. M. *Coord. Chem. Rev.* **2003**, *238*, 55.
(51) Aldridge, S.; Rossin, A.; Coombs, D. L.; Willock, D. J. *Dalton Trans.* **2004**, 2649.
(52) Pandey, K. K.; Lledós, A.; Maseras, F. *Organometallics* **2009**, *28*, 6442.
(53) Pandey, K. K.; Musaev, D. J. *Organometallics* **2010**, *29*, 142.

cationic GaI-containing system,[31,32] we set out to systematically investigate the nature of M−Ga bonds in cationic terminal gallylene complexes of the Group 8 metals (as a function of M, L, and X) via energy decomposition analyses (EDAs). To this end we report geometric and electronic structure calculations on 26 cationic terminal gallylene complexes $[(\eta^5\text{-}C_5H_5)(L)_2M(GaX)]^+$ (M = Fe, Ru, Os; Table 1). In carrying out these analyses, we intended to answer two questions; the first addresses the degree of ionic and covalent character of the M−Ga bonds, while the second addresses the extent of the M←Ga σ bonding and M→Ga π back-bonding contributions to these bonds. These factors are addressed not only as a function of the halogen substituent X but also as a function of the metal, M, and the ancillary ligand framework. As a point of reference, these studies sought to assess the validity of a simplistic Valence Bond interpretation of these compounds which features a M=Ga double bond.

Computational Method

Calculations have been carried out on compounds **I**−**XXVI** at the nonlocal Density Functional Theory (DFT) level of theory using the exchange functional of Becke[54] and the correlation functional of Perdew[55] (BP86). Scalar relativistic effects have been considered using the ZORA formalism.[56] Uncontracted Slater-type orbitals (STOs) using triple-ζ basis sets augmented by two sets of polarization functions were employed for the SCF calculations.[57] The following core electrons were treated by the frozen-core approximation: $(1s)^2$ (C, N, O); $(1s2s2p)^{10}$ (P, Cl, Fe); $(1s2s2p3s3p)^{18}$ (Ga, Br); $(1s2s2p3s3p3d)^{28}$ (Ru); $(1s2s2p3s3p3d4s4p)^{36}$ (I); $(1s2s2p3s3p3d4s4p4d)^{46}$ (Os).[58] An auxiliary set of s, p, d, f, and g STOs was used to fit the molecular densities and to present the Coulomb and exchange potentials accurately in each SCF cycle.[59] The calculations were performed utilizing the program package ADF-2009.01.[60] The binding interactions between the metal fragments $[(\eta^5\text{-}C_5H_5)(L)_2M]^+$ (singlet state) and GaX fragments (singlet state) were analyzed in C_s symmetry using the energy decomposition scheme of ADF which is based on the methods of Morokuma and Ziegler and Rauk.[61,62] The bond energy ΔE between fragments is separated into two major components ΔE_{int} and ΔE_{prep}:

$$\Delta E = \Delta E_{int} + \Delta E_{prep} \quad (1)$$

Table 1. Complexes of the Type $[(\eta^5\text{-}C_5H_5)(L)_2M(GaX)]^+$ Investigated in the Current Study

compound	M	L	X
I	Fe	CO	Cl
II	Fe	CO	Br
III	Fe	CO	I
IV	Fe	CO	NMe_2
V	Fe	CO	Mes
VI	Fe	PMe_3	Cl
VII	Fe	PMe_3	Br
VIII	Fe	PMe_3	I
IX	Fe	PMe_3	NMe_2
X	Fe	PMe_3	Mes
XI	Ru	CO	Cl
XII	Ru	CO	Br
XIII	Ru	CO	I
XIV	Ru	CO	NMe_2
XV	Ru	CO	Mes
XVI	Ru	PMe_3	I
XVII	Ru	PMe_3	NMe_2
XVIII	Ru	PMe_3	Mes
XIX	Os	CO	Cl
XX	Os	CO	Br
XXI	Os	CO	I
XXII	Os	CO	NMe_2
XXIII	Os	CO	Mes
XXIV	Os	PMe_3	I
XXV	Os	PMe_3	NMe_2
XXVI	Os	PMe_3	Mes

where ΔE_{prep} is the energy required to promote the structures of the free fragments from their equilibrium structure in the electronic ground state to the geometry and electronic state which they take up in the molecule, that is,

$$\Delta E_{prep} = E_{total}(\text{distorted fragments}) - E_{total}(\text{fragments in the equilibrium structure}) \quad (2)$$

ΔE_{int} in eq 1 is the instantaneous interaction energy between the two fragments in the molecule. It can be decomposed into three main components according to:

$$\Delta E_{int} = \Delta E_{elstat} + \Delta E_{Pauli} + \Delta E_{orb} \quad (3)$$

ΔE_{elstat} describes the classical Coulombic interaction between the fragments which is attractive in most cases. The term ΔE_{Pauli}, which is called exchange repulsion or Pauli repulsion, takes into account the destabilizing two-orbital, three- or four-electron interactions between occupied orbitals of both fragments. ΔE_{Pauli} is calculated by enforcing the Kohn−Sham determinant of the molecule, which results from superimposing both fragments, to obey the Pauli principle through antisymmetrization and renormalization. The last term ΔE_{orb} in eq 3 gives the stabilizing orbital interactions between occupied and virtual orbitals of the two fragments. ΔE_{orb} can be further partitioned into contributions from orbitals which belong to different irreducible representations of the point group of the system. It has been suggested that the covalent and electrostatic character of a bond is given by the ratio $\Delta E_{elstat}/\Delta E_{orb}$.[48−50,63−65] The electronic structures of the complexes were further examined by NBO analysis.[66] All molecular

(54) Becke, A. D. *Phys. Rev. A* **1988**, *38*, 3098.
(55) Perdew, J. P. *Phys. Rev. B* **1986**, *33*, 8822.
(56) (a) Chang, C.; Pelissier, M.; Durand, Ph. *Phys. Scr.* **1986**, *34*, 394. (b) Heully, J.-L.; Lindgren, I.; Lindroth, E.; Lundquist, S.; Martensson-Pendrill, A.-M. *J. Phys. B* **1986**, *19*, 2799. (c) van Lenthe, E.; Baerends, E. J.; Snijders, J. G. *J. Chem. Phys.* **1993**, *99*, 4597. (d) van Lenthe, E.; Baerends, E. J.; Snijders, J. G. *J. Chem. Phys.* **1996**, *105*, 6505. (e) van Lenthe, E.; van Leeuwen, R.; Baerends, E. J.; Snijders, J. G. *Int. J. Quantum Chem.* **1996**, *57*, 281. (f) van Lenthe, E.; Ehlers, A. E.; Baerends, E. J. *J. Chem. Phys.* **1999**, *110*, 8943.
(57) Snijders, J. G.; Baerends, E. J.; Vernooijs, P. *At. Data Nucl. Data Tables* **1982**, *26*, 483.
(58) Baerends, E. J.; Ellis, D. E.; Ros, P. *Chem. Phys.* **1973**, *2*, 41.
(59) Krijn, J.; Baerends, E. J. *Fit Functions in the HFS-Method, Internal Report (in Dutch)*; Vrije Universiteit Amsterdam: The Netherlands, 1984.
(60) Baerends, E. J.; Autschbach, J. A.; Berces, A.; Bo, C.; Boerrigter, P. M.; Cavallo, L.; Chong, D. P.; Deng, L.; Dickson, R. M.; Ellis, D. E.; Fan, L.; Fischer, T. H.; Fonseca Guerra, C.; van Gisbergen, S. J. A.; Groeneveld, J. A.; Gritsenko, O. V.; Grüning, M.; Harris, F. E.; van den Hoek, P.; Jacobsen, H.; van Kessel, G.; Kootstra, F.; van Lenthe, E.; Osinga, V. P.; Patchkovskii, S. Philipsen, P. H. T.; Post, D. Pye, C. C.; Ravenek, W.; Ros, P.; Schipper, P. R. T.; Schreckenbach, G.; Snijders, J. G.; Sola, M.; Swart, M.; Swerhone, D.; te Velde, G.; Vernooijs, P.; Versluis, L.; Visser, O.; Wezenbeek, E.; Wiesenekker, G.; Wolff, S. K.; Woo, T. K.; Ziegler, T. *ADF 2008−01*; Scientific Computing & Modelling NV: The Netherlands.
(61) (a) Morokuma, K. *J. Chem. Phys.* **1971**, *55*, 1236. (b) Morokuma, K. *Acc. Chem. Res.* **1977**, *10*, 294.
(62) (a) Ziegler, T.; Rauk, A. *Theor. Chim. Acta* **1977**, *46*, 1. (b) Ziegler, T.; Rauk, A. *Inorg. Chem.* **1979**, *18*, 1558. (c) Ziegler, T.; Rauk, A. *Inorg. Chem.* **1979**, *18*, 1755.
(63) Pandey, K. K. *Coord. Chem. Rev.* **2009**, *253*, 37.
(64) Pandey, K. K.; Lledós, A. *Inorg. Chem.* **2009**, *48*, 2748.
(65) Pandey, K. K.; Patidar, P.; Braunschweig, H. *Inorg. Chem.* **2010**, *49*, 6994.
(66) Reed, A. E.; Curtiss, L. A.; Weinhold, F. *Chem. Rev.* **1988**, *88*, 899.
(67) Schaftenaar, G. *MOLDEN3.4*; CAOSCAMM Center, :The Netherlands, 1998.

Table 2. Important Optimized Structural Parameters for the Cationic Gallylene Complexes $[(\eta^5\text{-}C_5H_5)(L)_2M(GaX)]^+$, **I**–**XXVI**

	bond distances (Å)				bond angles (deg)				
	M–Ga	Ga–R	M–CO	M–P	M–Ga–R	C–M–C	P–M–P	Ga–M–C	Ga–M–P
Iron-Gallylene Complexes									
$[(\eta^5\text{-}C_5H_5)(OC)_2Fe(GaCl)]^+$ **I**	2.235	2.102	1.774		178.0	94.0		91.6	
$[(\eta^5\text{-}C_5H_5)(OC)_2Fe(GaBr)]^+$ **II**	2.246	2.248	1.774		178.8	94.1		91.5	
$[(\eta^5\text{-}C_5H_5)(OC)_2Fe(GaI)]^+$ **III**	2.244	2.442	1.773		178.7	94.1		91.1	
$[(\eta^5\text{-}C_5H_5)(OC)_2Fe(GaNMe_2)]^+$ **IV**	2.252	1.796	1.767		177.4	93.8		90.2	
$[(\eta^5\text{-}C_5H_5)(OC)_2Fe(GaMes)]^+$ **V**	2.253	1.928	1.762		179.9	94.1		89.7	
$[(\eta^5\text{-}C_5H_5)(Me_3P)_2Fe(GaCl)]^+$ **VI**	2.192	2.145		2.249	175.2		98.7		91.8
$[(\eta^5\text{-}C_5H_5)(Me_3P)_2Fe(GaBr)]^+$ **VII**	2.203	2.297		2.249	178.9		98.7		92.2
$[(\eta^5\text{-}C_5H_5)(Me_3P)_2Fe(GaI)]^+$ [a] **VIII**	2.201	2.497		2.245	174.7		98.8		91.9
	2.2221(6)	2.4436(5)		2.214	171.37(3)				
$[(\eta^5\text{-}C_5H_5)(Me_3P)_2Fe(GaNMe_2)]^+$ **IX**	2.215	1.825		2.234	174.8		98.2		92.1
$[(\eta^5\text{-}C_5H_5)(Me_3P)_2Fe(GaMes)]^+$ **X**	2.214	1.966		2.228	172.9		98.3		93.3
Ruthenium-Gallylene Complexes									
$[(\eta^5\text{-}C_5H_5)(OC)_2Ru(GaCl)]^+$ **XI**	2.349	2.103	1.907		177.3	91.5		90.3	
$[(\eta^5\text{-}C_5H_5)(OC)_2Ru(GaBr)]^+$ **XII**	2.360	2.249	1.906		178.1	91.4		90.0	
$[(\eta^5\text{-}C_5H_5)(OC)_2Ru(GaI)]^+$ **XIII**	2.358	2.442	1.905		177.8	91.5		89.8	
$[(\eta^5\text{-}C_5H_5)(OC)_2Ru(GaNMe_2)]^+$ **XIV**	2.365	1.796	1.897		177.9	91.2		89.2	
$[(\eta^5\text{-}C_5H_5)(OC)_2Ru(GaMes)]^+$ **XV**	2.368	1.926	1.894		179.7	91.5		88.6	
$[(\eta^5\text{-}C_5H_5)(Me_3P)_2Ru(GaI)]^+$ **XVI**	2.306	2.494		2.338	174.6		97.6		90.9
$[(\eta^5\text{-}C_5H_5)(Me_3P)_2Ru(GaNMe_2)]^+$ **XVII**	2.323	1.823		2.327	172.5		96.9		91.9
$[(\eta^5\text{-}C_5H_5)(Me_3P)_2Ru(GaMes)]^+$ **XVIII**	2.318	1.963		2.321	171.7		96.9		92.8
Osmium-Gallylene Complexes									
$[(\eta^5\text{-}C_5H_5)(OC)_2Os(GaCl)]^+$ **XIX**	2.362	2.097	1.910		176.4	91.3		90.0	
$[(\eta^5\text{-}C_5H_5)(OC)_2Os(GaBr)]^+$ **XX**	2.374	2.243	1.909		177.0	91.3		90.0	
$[(\eta^5\text{-}C_5H_5)(OC)_2Os(GaI)]^+$ **XXI**	2.372	2.435	1.908		176.9	91.3		89.7	
$[(\eta^5\text{-}C_5H_5)(OC)_2Os(GaNMe_2)]^+$ **XXII**	2.381	1.792	1.903		176.8	90.9		89.6	
$[(\eta^5\text{-}C_5H_5)(Me_3P)_2Os(GaMes)]^+$ **XXIII**	2.387	1.922	1.899		178.3	91.3		88.6	
$[(\eta^5\text{-}C_5H_5)(Me_3P)_2Os(GaI)]^+$ **XXIV**	2.325	2.486		2.343	173.0		97.7		90.9
$[(\eta^5\text{-}C_5H_5)(Me_3P)_2Os(GaNMe_2)]^+$ **XXV**	2.339	1.819		2.333	170.4		97.0		92.0
$[(\eta^5\text{-}C_5H_5)(Me_3P)_2Os(GaMes)]^+$ **XXVI**	2.337	2.957		2.328	171.1		96.9		92.6

[a] X-ray structure data for $[(\eta^5\text{-}C_5Me_5)(dppe)Fe(GaI)]^+[BAr^f_4]^-$.[31,32]

orbital pictures were produced using the MOLDEN program.[67]

Results and Discussion

Geometries. The important bond distances and angles of metal gallylene complexes **I**–**XXVI** calculated at the BP86/TZ2P level of theory are presented in Table 2. Geometric structures are shown in Figure 1 for the cases where M = Fe (general geometric features of the ruthenium and osmium complexes are very similar and are therefore not included in the figure). The optimized Cartesian coordinates of all complexes are given in the Supporting Information. Although half-sandwich ruthenium and osmium gallylene complexes are not known, the calculated geometric parameters of the model iron gallylene complex $[(\eta^5\text{-}C_5H_5)(Me_3P)_2Fe(GaI)]^+$ are in excellent agreement with the experimental values available for $[(\eta^5\text{-}C_5Me_5)(dppe)Fe(GaI)]^+[BAr^f_4]^-$.[31,32]

As summarized in Table 2, the M–Ga bond distances determined computationally for complexes **I**–**XII** are significantly shorter than expected for M–Ga single bonds estimated on the basis of covalent radius predictions (2.40, 2.49, and 2.53 Å for Fe–Ga, Ru–Ga, and Os–Ga, respectively), but, for ruthenium and osmium at least, slightly longer than expected for M=Ga double bonds (2.26, 2.31, 2.33 Å for Fe=Ga, Ru=Ga, and Os=Ga).[68] The Fe–Ga distances for GaI complexes **III** and **VII** (2.244 and 2.201 Å) are relatively short on this basis, but are comparable, not only to that measured for $[(\eta^5\text{-}C_5Me_5)(dppe)Fe(GaI)]^+$ [2.2221(6) Å] but also to the bond lengths predicted for the charge neutral complexes $(OC)_4Fe(GaI)$ (axial isomer: 2.226 Å; equatorial isomer 2.229 Å).[46b] On substitution of the CO ancillary ligands by the less π-acidic PMe_3, the calculated M–Ga bond distances decrease [e.g., from 2.244 (**III**) to 2.201 Å (**VIII**); 2.358 (**XIII**) to 2.306 Å (**XVI**); and 2.372 (**XXI**) to 2.325 Å (**XXIV**) for the iodogallylene complexes $[(\eta^5\text{-}C_5H_5)(L)_2M(GaI)]^+$ (M = Fe, Ru, Os, respectively)], consistent with the metal center in each case becoming more electron rich (Figure 2).

The gallium bound substituent also exerts an influence on the calculated M–Ga bond distances, albeit a relatively small one. Thus, for each of the four series of compounds encompassing the complete range of substituents (X = Cl, Br, I, NMe_2, Mes) a slight increase in the M–Ga distance is found on going from X = Cl to X = Br or I (which are themselves very similar), with a further increase being observed for the $GaNMe_2$ and GaMes complexes (Table 2).

A number of factors are likely to influence these geometric parameters, including:

(i) The degree of gallium s character in the M–Ga bond. Thus, for the complexes $[(\eta^5\text{-}C_5H_5)(OC)_2Fe(GaCl)]^+$ [d(Fe–Ga) = 2.235 Å] and

(68) Pyykkö, P.; Atsumi, M. *Chem.—Eur. J.* **2009**, *15*, 12770.

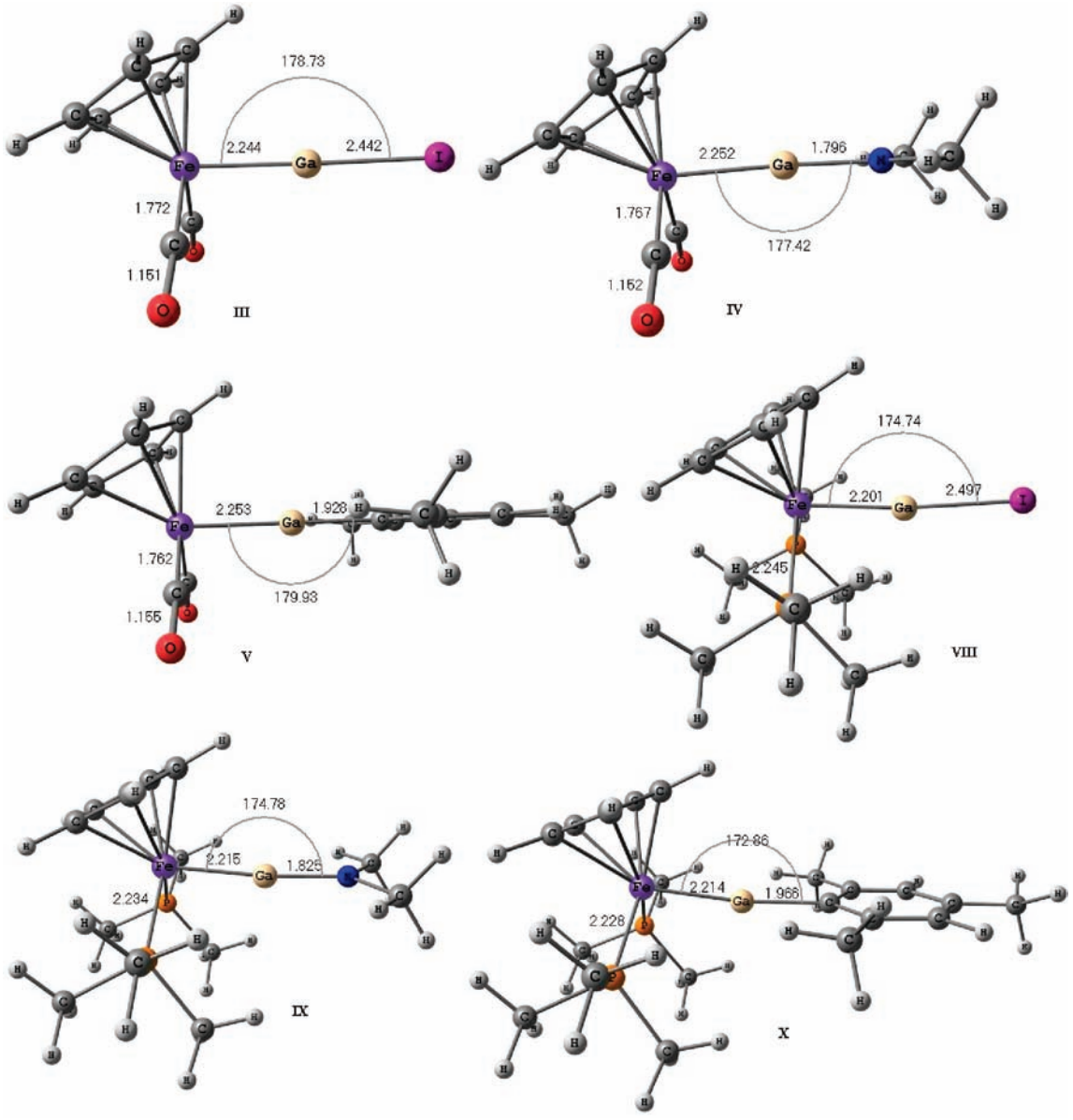

Figure 1. Optimized geometries of the iron gallylene complexes $[(\eta^5\text{-}C_5H_5)(L)_2Fe(GaX)]^+$ (L = CO, PMe_3; X = I, NMe_2, Mes); important bond lengths and angles are given in Table 1.

$[(\eta^5\text{-}C_5H_5)(OC)_2Fe(GaMes)]^+$ [d(Fe−Ga) = 2.253 Å] the % gallium s character decreases from 60.9 to 50.9% (with a concomitant increase in the contribution to the Ga−X linkage of 39.1 to 49.1%). At a more general level, it is this relatively high gallium s character in the M−Ga bonds which is thought to be responsible for the short M−Ga distances, rather than any great degree of M to Ga π back-bonding (vide infra).

(ii) Electrostatic contributions to the M−Ga bond; in all cases the M−Ga bond is marginally shorter for the GaCl complex than for GaI. The polarization of the bond in the sense $M^{\delta-}-Ga^{\delta+}$ (and the consequent electrostatic attraction) becomes smaller as the halogen substituent becomes less electronegative [e.g., NPA charges (Fe/Ga/X) of −1.50/+1.34/−0.37 for GaCl complex **I**; −1.47/+1.08/−0.10 for GaI complex **III**; Table 3].

(iii) The natures of the highest occupied molecular orbitals (HOMOs) and lowest unoccupied molecular orbitals (LUMOs) of the GaX and $[(\eta^5\text{-}C_5H_5)(L)_2M(GaX)]^+$ fragments (Figure 3) and their effects on M−Ga σ- and π- orbital interactions. Thus, for example, the HOMOs of the fragments $[(\eta^5\text{-}C_5H_5)(Me_3P)_2M]^+$ are higher in energy than the corresponding MOs for $[(\eta^5\text{-}C_5H_5)(OC)_2M]^+$ and therefore match more closely in energy the LUMO of the [GaX] fragments, thereby allowing for better $[(\eta^5\text{-}C_5H_5)(Me_3P)_2\text{-}M]^+\rightarrow$[GaX] back-donation. As a consequence, the absolute magnitudes of the π symmetry orbital contributions (ΔE_π) between the two fragments are somewhat higher for bis(phosphine) complexes compared to the related dicarbonyl-ligated systems (e.g., −13.9 vs −7.7 kcal mol^{-1} for Fe−GaI complexes **VII** and **III**).

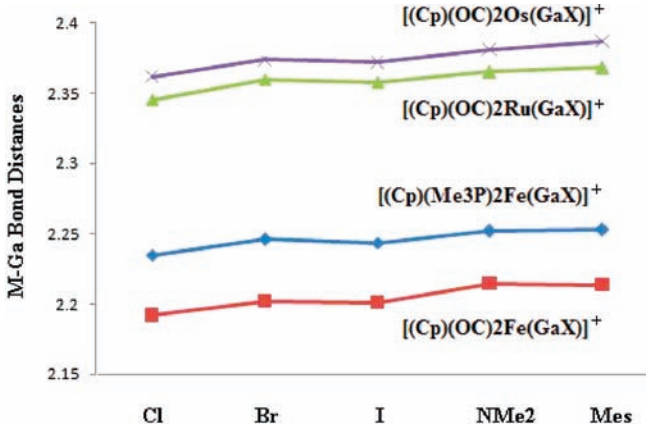

Figure 2. Variation in M−Ga bond distances in the complexes $[(\eta^5\text{-}C_5H_5)(OC)_2Fe(GaX)]^+$, $[(\eta^5\text{-}C_5H_5)(Me_3P)_2Fe(GaX)]^+$, $[(\eta^5\text{-}C_5H_5)(OC)_2Ru(GaX)]^+$, and $[(\eta^5\text{-}C_5H_5)(OC)_2Os(GaX)]^+$.

Table 3. Wiberg Bond Indices (WBIs), NPA Charges, and NBO Analyses for the M−Ga Bonds in the Cationic Gallylene Complexes $[(\eta^5\text{-}C_5H_5)(L)_2M(GaX)]^+$, **I**−**XXVI**

	Wiberg bond indices					NPA charges							M−Ga bond		
	M−Ga	Ga−R	M−P	M−CO	C−O	M	Ga	R	GaX	Cp	CO	PMe_3	Occu.	%M	%Ga
Iron-Gallylene Complexes															
$[(\eta^5\text{-}C_5H_5)(OC)_2Fe(GaCl)]^+$ **I**	0.80	0.88		1.04	2.23	−1.50	1.34	−0.37	0.97	0.67	0.43		1.516	47.40	52.60
$[(\eta^5\text{-}C_5H_5)(OC)_2Fe(GaBr)]^+$ **II**	0.78	1.02		1.04	2.23	−1.48	1.21	−0.25	0.96	0.68	0.42		1.520	46.70	53.30
$[(\eta^5\text{-}C_5H_5)(OC)_2Fe(GaI)]^+$ **III**	0.76	1.15		1.04	2.22	−1.47	1.08	−0.10	0.98	0.65	0.42		1.513	46.29	53.71
$[(\eta^5\text{-}C_5H_5)(OC)_2Fe(GaNMe_2)]^+$ **IV**	0.78	0.68		1.06	2.20	−1.49	1.51	−0.38	1.13	0.56	0.40		1.722	66.35	33.65
$[(\eta^5\text{-}C_5H_5)(OC)_2Fe(GaMes)]^+$ **V**	0.70	0.61		1.07	2.18	−1.51	1.50	−0.33	1.17	0.56	0.39		1.692	71.37	28.63
$[(\eta^5\text{-}C_5H_5)(Me_3P)_2Fe(GaCl)]^+$ **VI**	0.97	0.75	0.81			−1.67	1.27	−0.46	0.81	0.44		0.71	1.799	41.73	58.27
$[(\eta^5\text{-}C_5H_5)(Me_3P)_2Fe(GaBr)]^+$ **VII**	0.95	0.88	0.81			−1.65	1.16	−0.35	0.81	0.44		0.70	1.773	38.68	61.32
$[(\eta^5\text{-}C_5H_5)(Me_3P)_2Fe(GaI)]^{+b}$ **VIII**	0.93	1.00	0.81			−1.66	1.04	−0.22	0.82	0.44		0.70	1.771	37.32	62.68
$[(\eta^5\text{-}C_5H_5)(Me_3P)_2Fe(GaNMe_2)]^+$ **IX**	0.94	0.51	0.82			−1.72	1.51	−0.56	0.95	0.40		0.68	1.705	44.44	55.56
$[(\eta^5\text{-}C_5H_5)(Me_3P)_2Fe(GaMes)]^+$ **X**	0.86	0.49	0.82			−1.75	1.50	−0.46	1.04	0.35		0.68	1.889	57.51	42.29
Ruthenium-Gallylene Complexes															
$[(\eta^5\text{-}C_5H_5)(OC)_2Ru(GaCl)]^+$ **XI**	0.76	0.89		1.11	2.23	−1.37	1.35	−0.37	0.98	0.57	0.41		1.503	47.11	52.89
$[(\eta^5\text{-}C_5H_5)(OC)_2Ru(GaBr)]^+$ **XII**	0.75	1.02		1.11	2.23	−1.34	1.22	−0.25	0.97	0.55	0.41		1.584	51.16	48.84
$[(\eta^5\text{-}C_5H_5)(OC)_2Ru(GaI)]^+$ **XIII**	0.73	1.15		1.11	2.22	−1.34	1.10	−0.11	0.99	0.55	0.40				
$[(\eta^5\text{-}C_5H_5)(OC)_2Ru(GaNMe_2)]^+$ **XIV**	0.75	0.70		1.13	2.20	−1.35	1.51	−0.46	1.05	0.52	0.39		1.695	46.94	53.06
$[(\eta^5\text{-}C_5H_5)(OC)_2Ru(GaMes)]^+$ **XV**	0.68	0.62		1.14	2.19	−1.36	1.51	−0.34	1.17	0.45	0.37				
$[(\eta^5\text{-}C_5H_5)(Me_3P)_2Ru(GaI)]^+$ **XVI**	0.86	1.01	0.79			−1.69	1.06	−0.23	0.83	0.40		0.73	1.530	47.18	52.82
$[(\eta^5\text{-}C_5H_5)(Me_3P)_2Ru(GaNMe_2)]^+$ **XVII**	0.87	0.54	0.80			−1.74	1.51	−0.55	0.96	0.35		0.72	1.895	56.64	43.36
$[(\eta^5\text{-}C_5H_5)(Me_3P)_2Ru(GaMes)]^+$ **XVIII**	0.80	0.52	0.81			−1.77	1.51	−0.45	1.06	0.33		0.69			
Osmium-Gallylene Complexes															
$[(\eta^5\text{-}C_5H_5)(OC)_2Os(GaCl)]^+$ **XIX**	0.83	0.92		1.23	2.19	−1.27	1.36	−0.36	1.00	0.55	0.37		1.777	63.57	36.43
$[(\eta^5\text{-}C_5H_5)(OC)_2Os(GaBr)]^+$ **XX**	0.82	1.05		1.23	2.19	−1.25	1.23	−0.24	0.99	0.52	0.37		1.893	54.63	45.37
$[(\eta^5\text{-}C_5H_5)(OC)_2Os(GaI)]^+$ **XXI**	0.80	1.18		1.23	2.18	−1.24	1.10	−0.10	1.00	0.52	0.36		1.892	54.05	45.95
$[(\eta^5\text{-}C_5H_5)(OC)_2Os(GaNMe_2)]^+$ **XXII**	0.81	0.73		1.25	2.17	−1.25	1.52	−0.45	1.07	0.50	0.34		1.869	59.53	40.47
$[(\eta^5\text{-}C_5H_5)(OC)_2Os(GaMes)]^+$ **XXIII**	0.73	0.65		1.26	2.15	−1.27	1.51	−0.33	1.18	0.43	0.33		1.728	71.30	28.70
$[(\eta^5\text{-}C_5H_5)(Me_3P)_2Os(GaI)]^+$ **XXIV**	0.94	1.04	0.87			−1.68	1.04	−0.21	0.83	0.38		0.74	1.925	52.05	47.95
$[(\eta^5\text{-}C_5H_5)(Me_3P)_2Os(GaNMe_2)]^+$ **XXV**	0.94	0.58	0.88			−1.73	1.49	−0.54	0.95	0.35		0.72	1.682	46.16	53.84
$[(\eta^5\text{-}C_5H_5)(Me_3P)_2Os(GaMes)]^+$ **XXVI**	0.88	0.55	0.89			−1.76	1.48	−0.46	1.02	0.32		0.71	1.728	50.69	49.31

The optimized Ga−X bond distances in complexes **I**−**XXVI** are also shorter than would be expected for a single bond based on covalent radii predictions (2.23, 2.38, 2.57, 1.95, 1.99 Å for GaCl, GaBr, GaI, GaN, and GaC, respectively).[68] Moreover, the nature of the auxiliary ligand set strongly affects the Ga−X bond. Indeed, on replacing the CO ligand by PMe_3 (e.g., on going from complexes **I**−**V** to **VI**−**X**, the Ga−X bond of corresponding complexes is elongated by ca. 0.03 Å). The HOMOs of the metal fragments $[(\eta^5\text{-}C_5H_5)(Me_3P)_2M]^+$ are found closer in energy to the LUMO of [GaX], thereby allowing for better $[(\eta^5\text{-}C_5H_5)(PMe_3)_2M]^+ \rightarrow [GaX]$ π-donation to a [GaX] antibonding orbital. Thus, the Ga−X bond is relatively weaker in complexes of the type $[(\eta^5\text{-}C_5H_5)(Me_3P)_2M(GaX)]^+$ than in $[(\eta^5\text{-}C_5H_5)(OC)_2M(GaX)]^+$.

Bonding Analyses. We begin the analyses of M−Ga bonding in complexes **I**−**XXVI** with a discussion of bond orders and atomic charges. In Table 3 we present the calculated Wiberg Bond Indices (WBIs),[69] NPA charges, and the results of the natural bond orbital (NBO) analysis.

The WBIs for the M−Ga bonds of **I**−**XXVI** fall in the range 0.68−0.97, and thus suggest significant covalent

(69) Wiberg, K. B. *Tetrahedron* **1968**, *24*, 1083.

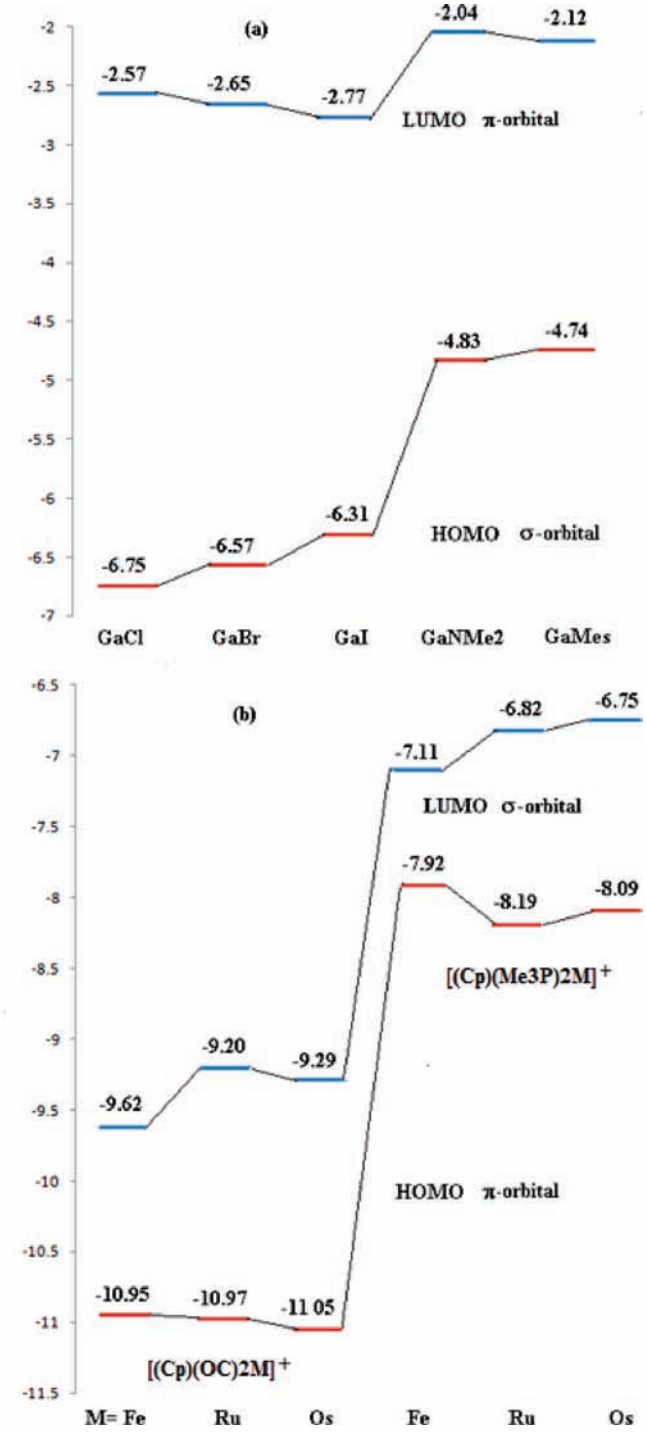

Figure 3. Frontier orbital energies (eV) of (a) ligands GaX; and (b) $[(\eta^5\text{-}C_5H_5)(L)_2M]^+$.

contributions to the M−Ga bonds. Moreover, upon substitution of the ancillary CO ligands by PMe_3, the M−Ga WBIs consistently increase (in a manner consistent with the decrease in calculated M−Ga bond lengths), for example, 0.88 and 0.97 for **I** and **VI**; 0.76 and 0.93 for **III** and **VIII**, respectively. By means of comparison, it is significant to note that the WBIs for the M−Ga bonds are markedly smaller than those for M−(CO) bonds; that is, the M−GaX bonds in complexes **I**−**XXVI** are weaker than M−CO bonds. The WBIs for the Ga−X bonds are slightly larger for complexes $[(\eta^5\text{-}C_5H_5)(OC)_2M(GaX)]^+$ than their $[(\eta^5\text{-}C_5H_5)(Me_3P)_2M(GaX)]^+$ counterparts, again consistent with the observed trend in the Ga−X distances.

Table 4. Results of NBO Analyses of the Cationic Iron Gallylene Complexes $[(\eta^5\text{-}C_5H_5)(OC)_2Fe(GaX)]^+$, **I**−**V**

	$[(\eta^5\text{-}C_5H_5)(CO)_2Fe(GaX)]^+$				
	Cl	Br	I	N(NMe_2)	C(Mes)
			M−Ga σ-Bond		
occupation	1.516	1.520	1.513	1.722	1.692
%M	47.40	46.70	46.29	66.35	71.37
%s	10.82	10.90	10.77	21.43	21.32
%p	76.36	76.29	76.51	23.99	22.67
%d	12.81	12.82	12.71	54.58	56.01
%f	0.00	0.00	0.00	0.00	0.00
Ga					
%Ga	52.60	53.30	53.71	33.65	28.63
%s	60.99	61.65	62.33	56.09	50.89
%p	38.91	38.29	37.64	43.33	48.55
%d	0.10	0.06	0.03	0.57	0.56
			Ga−X σ-Bond		
occupation	1.926	1.913	1.893	1.911	1.836
%Ga	19.09	23.10	28.14	14.07	22.70
%s	39.77	39.21	38.21	43.78	49.23
%p	59.82	60.49	60.85	55.76	50.53
%d	0.41	0.30	0.94	0.46	0.24
X					
%X	80.91	76.90	71.86	85.93	77.30
%s	17.33	14.49	12.25	24.33	19.85
%p	82.43	85.26	87.61	75.67	80.14
%d	0.24	0.25	0.14	0.01	0.01

The calculated natural (NPA) charge distributions indicate that the transition metal atom and X groups possess overall negative charges in complexes **I**−**XXVI**, while the gallium atom (and the GaX ligand in totality), Cp and CO groups are positively charged; the gallium center carries a large positive charge in all cases (+1.04 to +1.51). Substitution of the ancillary CO ligands by poorer π-acceptor/better σ-donor PMe_3 ligands, leads to a net increase in the magnitude of the negative charge at the metal atom (e.g., −1.50/−1.47 and −1.67/−1.66 for **I**/**III** and **VI**/**VIII**, respectively). In general, therefore, the electrostatic attraction between the gallium atom of the GaX ligand and metal atom of the $[(\eta^5\text{-}C_5H_5)(L)_2M]^+$ fragment and gallium atom of the GaX ligand increases on going from L = CO to L = PMe_3 [e.g., NPA charges (Fe/Ga) of −1.50/+1.34 for complex **I**; −1.67/+1.27 for complex **IV**, and corresponding values of −69.2, −85.3 kcal mol^{-1} for ΔE_{elstat}].

A more definitive picture of M−Ga bonding is obtained through NBO analysis of the delocalized Kohn−Sham orbitals. The characteristics of the M−Ga σ-bonding orbitals are summarized in Table 3. In most of the iron gallylene complexes **I**−**X**, the M−Ga σ-bonding orbital is polarized toward the gallium atom (i.e., the gallium center contributes more to the bonding orbital); the occupations of the M−Ga σ-bonding orbitals fall in the range 1.513−1.925. A detailed NBO analysis of the Fe−Ga and Ga−X bonds in the $[(\eta^5\text{-}C_5H_5)(OC)_2Fe(GaX)]^+$ (i.e., **I**−**V**) is presented in Table 4. It is important to note that gallium atom contributions to the M−Ga σ bonds reflect smaller p character (38.91% in **I**, 38.21% in **II**, 37.64% in **III**, 43.78% in **IV**, and 49.23% in **V**), while the Ga−X σ bonds have significantly larger p character (59.82% in **I**, 60.49% in **II**, 60.84 in **III**, 55.76% in **IV**, and 50.53% in **V**), in keeping with the tenets of Bent's Rule. [70]

Table 5. EDAs for the Cationic Gallylene Complexes $[(\eta^5\text{-}C_5H_5)(L)_2M(GaX)]^+$, **I**−**XXVI**.[a]

	ΔE_{int}	ΔE_{Pauli}	ΔE_{elstat}[b]		ΔE_{orb}	$\Delta E_{\sigma}(a')$	$\Delta E_{\pi}(a'')$[c]		ΔE_{prep}	ΔE(−BDE) M−GaX	ΔE(−BDE) M−CO[d]
Iron-Gallylene Complexes											
$[(\eta^5\text{-}C_5H_5)(OC)_2Fe(GaCl)]^+$ **I**	−49.0	101.7	−69.2	(45.9%)	−81.5	−73.8	−7.7	(9.4%)	3.7	−45.3	−65.8
$[(\eta^5\text{-}C_5H_5)(OC)_2Fe(GaBr)]^+$ **II**	−50.4	99.1	−66.6	(46.9%)	−82.9	−75.3	−7.6	(9.2%)	3.5	−46.9	−66.1
$[(\eta^5\text{-}C_5H_5)(OC)_2Fe(GaI)]^+$ **III**	−53.7	102.8	−68.9	(44.0%)	−87.6	−79.9	−7.7	(8.8%)	4.1	−53.6	−66.5
$[(\eta^5\text{-}C_5H_5)(OC)_2Fe(GaNMe_2)]^+$ **IV**	−67.4	117.4	−96.5	(52.2%)	−88.3	−80.8	−7.5	(8.5%)	4.0	−63.4	
$[(\eta^5\text{-}C_5H_5)(OC)_2Fe(GaMes)]^+$ **V**	−86.9	142.8	−123.0	(53.5%)	−106.7	−98.2	−8.5	(8.0%)	5.1	−81.8	
$[(\eta^5\text{-}C_5H_5)(Me_3P)_2Fe(GaCl)]^+$ **VI**	−38.9	120.4	−85.3	(53.5%)	−74.0	−60.2	−13.8	(18.6%)	4.8	−34.1	
$[(\eta^5\text{-}C_5H_5)(Me_3P)_2Fe(GaBr)]^+$ **VII**	−39.5	116.7	−82.2	(52.6%)	−74.0	−60.4	−13.6	(18.4%)	4.7	−34.8	
$[(\eta^5\text{-}C_5H_5)(Me_3P)_2Fe(GaI)]^+$[b] **VIII**	−41.2	120.5	−84.6	(52.3%)	−77.1	−63.2	−13.9	(18.2%)	4.9	−36.2	
$[(\eta^5\text{-}C_5H_5)(Me_3P)_2Fe(GaNMe_2)]^+$ **IX**	−49.6	133.0	−107.3	(58.8%)	−75.3	−62.4	−12.9	(17.1%)	5.2	−44.4	
$[(\eta^5\text{-}C_5H_5)(Me_3P)_2Fe(GaMes)]^+$ **X**	−63.2	156.2	−131.3	(59.8%)	−88.1	−74.0	−14.1	(16.0%)	6.7	−57.5	
Ruthenium-Gallylene Complexes											
$[(\eta^5\text{-}C_5H_5)(OC)_2Ru(GaCl)]^+$ **XI**	−50.6	113.7	−84.8	(51.6%)	−79.6	−70.6	−9.0	(11.3%)	4.5	−46.1	−63.2
$[(\eta^5\text{-}C_5H_5)(OC)_2Ru(GaBr)]^+$ **XII**	−51.9	110.5	−81.7	(50.3%)	−80.8	−72.0	−8.8	(10.9%)	4.4	−47.5	−63.4
$[(\eta^5\text{-}C_5H_5)(OC)_2Ru(GaI)]^+$ **XIII**	−55.2	114.4	−84.5	(49.9%)	−85.0	−76.1	−8.9	(10.5%)	5.1	−50.1	−63.9
$[(\eta^5\text{-}C_5H_5)(OC)_2Ru(GaNMe_2)]^+$ **XIV**	−54.6	147.2	−127.1	(63.0%)	−74.7	−61.8	−12.9	(17.3%)	2.3	−52.3	
$[(\eta^5\text{-}C_5H_5)(OC)_2Ru(GaMes)]^+$ **XV**	−68.9	128.9	−112.4	(56.8%)	−85.4	−76.9	−8.5	(10.0%)	5.0	−63.9	
$[(\eta^5\text{-}C_5H_5)(Me_3P)_2Ru(GaI)]^+$ **XVI**	−88.1	155.4	−141.6	(58.1%)	−102.0	−92.7	−9.3	(9.1%)	6.6	−81.5	
$[(\eta^5\text{-}C_5H_5)(Me_3P)_2Ru(GaNMe_2)]^+$ **XVII**	−45.9	136.2	−104.7	(57.5%)	−77.3	−63.0	−14.3	(18.5%)	6.1	−39.8	
$[(\eta^5\text{-}C_5H_5)(Me_3P)_2Ru(GaMes)]^+$ **XVIII**	−68.7	175.1	−156.2	(64.1%)	−87.6	−73.5	−14.1	(16.1%)	7.5	−61.2	
Osmium-Gallylene Complexes											
$[(\eta^5\text{-}C_5H_5)(OC)_2Os(GaCl)]^+$ **XIX**	−59.4	136.4	−104.9	(53.6%)	−90.9	−81.2	−9.7	(10.7%)	5.0	−54.3	−72.7
$[(\eta^5\text{-}C_5H_5)(OC)_2Os(GaBr)]^+$ **XX**	−60.6	132.5	−101.2	(52.5%)	−91.4	−82.4	−9.5	(10.4%)	4.9	−55.7	−72.7
$[(\eta^5\text{-}C_5H_5)(OC)_2Os(GaI)]^+$ **XXI**	−63.8	136.8	−104.4	(52.0%)	−96.2	−86.6	−9.6	(10.0%)	5.5	−58.3	−73.0
$[(\eta^5\text{-}C_5H_5)(OC)_2Os(GaNMe_2)]^+$ **XXII**	−77.8	152.8	−134.8	(58.4%)	−95.9	−86.9	−9.0	(9.4%)	5.7	−72.1	
$[(\eta^5\text{-}C_5H_5)(OC)_2Os(GaMes)]^+$ **XXIII**	−97.1	182.7	−167.7	(59.9%)	−112.1	−102.4	−9.7	(8.7%)	6.7	−90.4	
$[(\eta^5\text{-}C_5H_5)(Me_3P)_2Os(GaI)]^+$ **XXIV**	−54.0	165.0	−129.6	(59.2%)	−89.4	−73.9	−15.5	(17.3%)	8.9	−45.1	
$[(\eta^5\text{-}C_5H_5)(Me_3P)_2Os(GaNMe_2)]^+$ **XXV**	−63.1	179.0	−155.2	(64.1%)	−86.9	−72.8	−14.1	(16.2%)	9.4	−53.7	
$[(\eta^5\text{-}C_5H_5)(Me_3P)_2Os(GaMes)]^+$ **XXVI**	−78.0	210.5	−188.7	(65.4%)	−99.8	−84.7	−15.1	(15.1%)	10.6	−67.4	

[a] Energy contributions in kcal mol^{-1}. [b] The values in parentheses are the percentage contributions of the total electrostatic interactions, reflecting the ionic character of the bond. [c] The values in parentheses are the percentage contributions of π bonding to the total orbital interactions ΔE_{orb}. [d] M−CO BDEs, i.e., those for $[(\eta^5\text{-}C_5H_5)(OC)_2M(GaX)]^+ \rightarrow [(\eta^5\text{-}C_5H_5)(OC)M(GaX)]^+ + CO$.

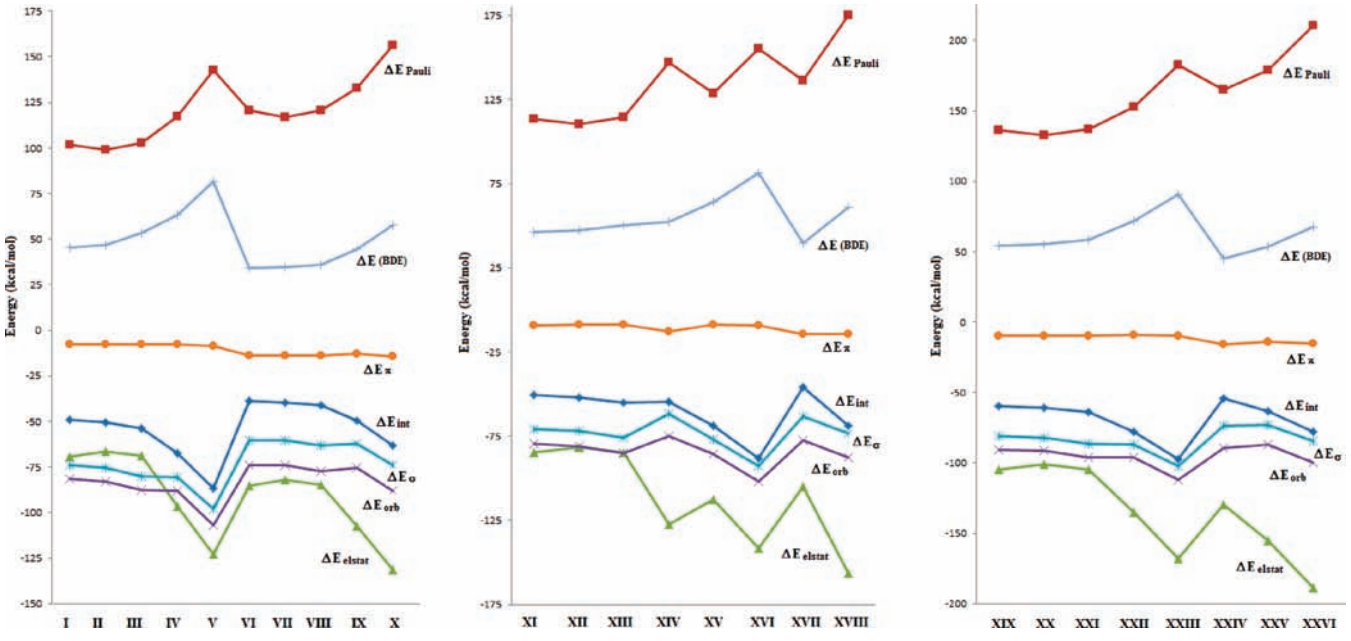

Figure 4. Values of the energy contributions to the M−Ga bonds in model complexes **I**−**XXVI**: Pauli repulsion (ΔE_{Pauli}), bond dissociation energy (BDE), interaction energy (ΔE_{int}), electrostatic interaction (ΔE_{elstat}, ionic contribution), orbital interaction (ΔE_{orb}, covalent contribution), σ- and π-symmetry orbial components (ΔE_{σ} and ΔE_{π}).

The Ga−X σ-bonding orbitals are largely polarized (72−86%) toward the X ligands. Moreover, these results reveal that the gallium atoms in the metal gallylene complexes are not sp-hybridized.

Energy Decomposition Analyses (EDAs). In addition to charge decomposition analyses at the NBO level, we have also carried out EDAs of the M−Ga bonds for **I**− **XXVI**; these results are summarized in Table 5 and Figure 4.

The tabulated bond dissociation energies (BDEs) reveal the expected periodic trend in the bond strengths due d-orbital extent/energy, that is, the Os−Ga bonds are stronger than the corresponding iron and ruthenium linkages. The interaction energies, ΔE_{int}, show the same trend as the calculated BDEs, with the discrepancies between the two values (i.e., ΔE_{prep}) amounting to about 5 kcal mol^{-1} in agreement with previous studies.[52] Figure 4 shows schematically the variation in BDE, Pauli repulsion (ΔE_{Pauli}), interaction energy (ΔE_{int}), electrostatic interaction (ΔE_{elstat}), and orbital interactions (ΔE_{orb}) for complexes **I**−**XXVI**, together with the σ- and π-bonding components (ΔE_{σ} and ΔE_{π}) of ΔE_{orb}. The breakdown of the interaction energy ΔE_{int} into the repulsive term ΔE_{Pauli} and the attractive terms ΔE_{orb} and ΔE_{elstat} shows that the ΔE_{Pauli} repulsive interactions have the larger absolute value for all complexes (Table 5). By means of comparison, the M−CO BDEs have also been calculated for the carbonyl containing complexes **I**− **III**, **XI**−**XIII**, and **XIX**−**XXI** (Table 5). In line with the calculated Wiberg bond indices and with recent bond energy analyses, the M−GaX bonds have lower BDEs than the corresponding M−CO linkages. Moreover, such a finding is in line with analyses reported by Frenking and co-workers for charge neutral complexes containing GaX ligands.[46]

Partitioning of the orbital interaction energies into ΔE_{σ} and ΔE_{π} gives insight into the magnitudes of the components of the orbital contribution to the interaction between $[(\eta^5\text{-}C_5H_5)(L)_2M]^+$ and [GaX] fragments. It is significant to note that the π-bonding contribution is, in all complexes studied, much smaller (8.0−18.6% of total orbital contributions) than the σ-bonding contribution. Relatively larger π-contributions are found for the bis(phosphine) complexes $[(\eta^5\text{-}C_5H_5)(Me_3P)_2M(GaX)]^+$ {e.g., 18.6 and 18.4% for $[(\eta^5\text{-}C_5H_5)(Me_3P)_2Fe(GaCl)]^+$, **VI**, and $[(\eta^5\text{-}C_5H_5)(Me_3P)_2Fe(GaI)]^+$, **VIII**, respectively} with a smaller π-contribution being observed for the corresponding dicarbonyl complexes {e.g., 9.4 and 8.8% for $[(\eta^5\text{-}C_5H_5)(OC)_2Fe(GaCl)]^+$, **I**, and $[(\eta^5\text{-}C_5H_5)(OC)_2Fe(GaI)]^+$, **III**, respectively}. The contribution of ΔE_{σ} is clearly the dominant term of the orbital interaction, and the EDA data thus suggest that these gallylene (GaX) ligands behave predominantly as σ-donors. A similar finding has been reported for both axial and equatorial isomers of the charge neutral complexes $(OC)_4Fe(GaX)$ (X = F−I) for which ΔE_{π} represents between 22.9 and 28.8% of the total orbital contribution.[46b]

Figure 3 shows the frontier orbital energies of the GaX ligands and of the metal fragments $[(\eta^5\text{-}C_5H_5)(L)_2M]^+$. The energies of the σ symmetry HOMOs are significantly higher for $GaNMe_2$ and GaMes compared to GaCl, GaBr, and GaI, implying that the $GaNMe_2$ and GaMes ligands are better σ-donors than the halogallylenes. This is reflected in higher BDEs for complexes **IV** and **V** (−63.4 and −81.8 kcal mol^{-1}) compared to **I**−**III** (−45.3, −46.9, and −53.6 kcal mol^{-1}). With regard to the metal fragment, the π-donor HOMO and σ-acceptor LUMO orbitals of $[(\eta^5\text{-}C_5H_5)(Me_3P)_2M]^+$ lie at markedly higher energies than those of the corresponding $[(\eta^5\text{-}C_5H_5)(OC)_2M]^+$ fragments. In particular, the LUMOs of the bis(phosphine) systems $[(\eta^5\text{-}C_5H_5)(Me_3P)_2M]^+$ lie closer in energy to the HOMOs of the $GaNMe_2$ and GaMes, and thereby allow for better donation and relatively stronger M−Ga σ bond interactions in $[(\eta^5\text{-}C_5H_5)(Me_3P)_2M(GaX)]^+$ (X = NMe_2, Mes).

The π-system of the Mes ring is a weak donor for the out-of-plane p(π) atomic orbital at gallium (Figure 5E), and the calculated bond energies for GaMes complexes are typically higher than for the other gallylene ligands GaX (X = Cl, Br, I, NMe_2). The ligand $GaNMe_2$ is nearly as strong a π-acceptor as GaMes (as manifested by ΔE_{π} values of 8.5 and 7.5 kcal mol^{-1} for **V** and **IV**, respectively), and yet, the M−GaMes bond energies are typically higher than those

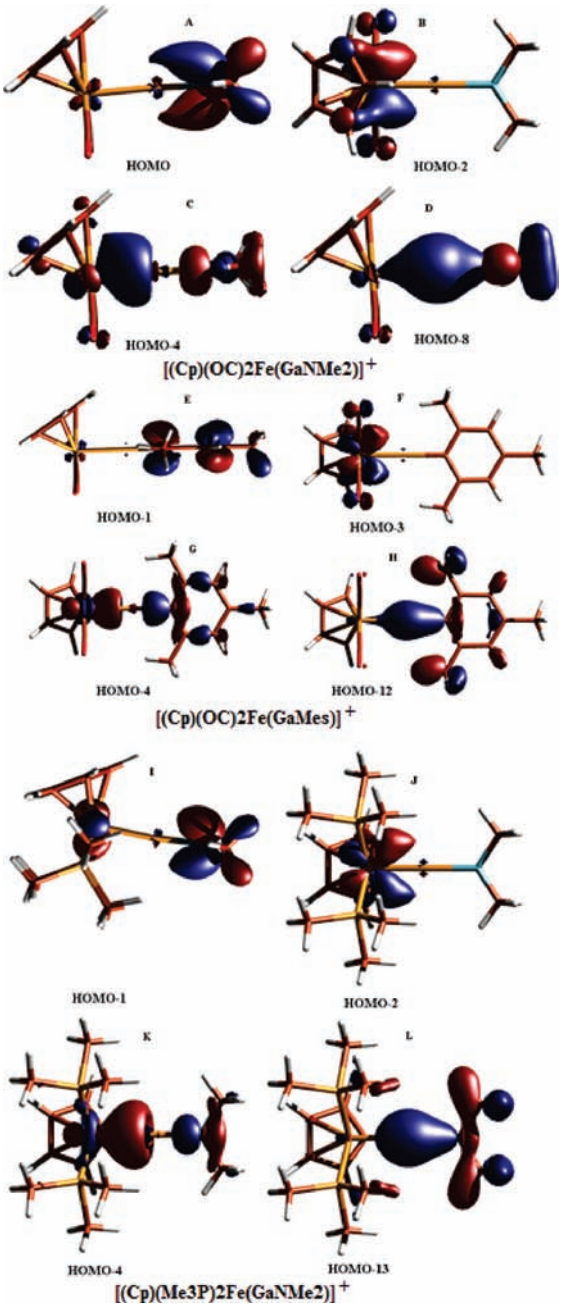

Figure 5. Plot of relevant molecular orbitals for $[(\eta^5\text{-}C_5H_5)(OC)_2Fe(GaNMe_2)]^+$, **IV**, $[(\eta^5\text{-}C_5H_5)(OC)_2Fe(GaMes)]^+$, **V**, and $[(\eta^5\text{-}C_5H_5)(Me_3P)_2Fe(GaNMe_2)]^+$, **IX**.

(70) Bent, H. A. *Chem. Rev.* **1961**, *61*, 275.

for M−GaNMe$_2$ bonds (e.g., −81.8 and −63.4 kcal mol^{-1} for **V** and **IV**). In this context, is significant to note that the total charge transfer $[(\eta^5\text{-}C_5H_5)(L)_2M]^+\leftarrow$GaX is always larger for X = Mes than for Cl, Br, I, or NMe$_2$ (Table 2). These results reveal that the M−GaMes bonds have greater ionic character (as manifested by ΔE_{Elstat} values of −123.0 and −96.5 kcal mol^{-1} for **V** and **IV**). In general, the contribution of the electrostatic interaction term ΔE_{elstat} to the M−GaX bonding is comparable to, or even slightly larger than the covalent bonding ΔE_{orb} term. Thus, for example, for the iron systems **I**−**X**, ΔE_{elstat} represents between 44.0 and 59.8% of ΔE_{int}, a finding in agreement with the behavior reported for the same GaX ligands in *charge neutral* complexes.[46b]

To visualize the M−Ga σ- and π- bonding and Ga−X σ- and π- bonding interactions, envelope plots of relevant orbitals of the iron gallylene complexes $[(\eta^5\text{-}C_5H_5)(OC)_2Fe(GaNMe_2)]$, **IV**, $[(\eta^5\text{-}C_5H_5)(OC)_2Fe(GaMes)]$, **V**, and $[(\eta^5\text{-}C_5H_5)(Me_3P)_2Fe(GaNMe_2)]$, **IX**, are given in Figure 5. Figures 5B, 5F, and 5J give pictorial descriptions of the respective Fe−Ga π symmetry orbital, with the very small gallium orbital contributions indicating weak Fe−Ga π interactions. By contrast, Figures 5C, 5G, and 5K show the Fe−Ga σ bonding orbitals, consistent with strong Fe−Ga σ interactions.

Conclusions

On the basis of quantum chemical studies of structure and bonding carried out on 26 model Group 8 gallylene complexes the following conclusions can be drawn:

(i) The M−Ga bonds in these systems are short, and are (marginally) shorter for GaCl than for GaBr and GaI complexes; such observations are consistent with a high degree of gallium s character in the M−Ga bond, and with a significant role for the electrostatic component of ΔE_{int}.

(ii) The π-bonding contribution (ΔE_π) is, in all complexes, smaller (8.0−18.6% of total orbital contributions) than the corresponding σ-bonding contribution. Relatively larger π-contributions (and shorter M−Ga bonds) are found for the complexes $[(\eta^5\text{-}C_5H_5)(Me_3P)_2M(GaX)]^+$ compared to $[(\eta^5\text{-}C_5H_5)(OC)_2M(GaX)]^+$, reflecting their markedly higher HOMO energies. Nevertheless, the contribution of ΔE_σ is clearly the dominant term of the orbital interaction, and GaX ligands are predominantly σ-donor ligands.

(iii) The Wiberg bond indices (WBIs) for the M−GaX and M−CO bonds indicate that the M−GaX bonds in the cationic gallylene complexes studied are weaker than M−CO bonds, as indeed has been shown experimentally for $[(\eta^5\text{-}C_5Me_5)(dppe)Fe(GaI)]^+$.[31,32]

(iv) The total charge transfer $[(\eta^5\text{-}C_5H_5)(L)_2M]^+\leftarrow$GaX is typically larger when X = Mes than when X = Cl, Br, I, or NMe$_2$; the M−GaX bonds in $[(\eta^5\text{-}C_5H_5)(L)_2M(GaMes)]^+$ thus have greater ionic character and typically larger BDEs.

(v) The BDEs of the M−Ga bonds in the complexes $[(\eta^5\text{-}C_5H_5)(OC)_2M(GaX)]^+$ (M = Fe, Ru, Os, X = Cl, Br, I, NMe$_2$, Mes) increase on going from X = Cl to Mes, and from X = Fe to Os. The contributions of the electrostatic interaction ΔE_{elstat} increase in the order M = Fe < Ru < Os.

Acknowledgment. S.A. thanks the EPSRC for funding (EP/F019181/1).

Supporting Information Available: Cartesian coordinates of the optimized geometries of metal gallylene complexes **I**−**XXVI**. This material is available free of charge via the Internet at http://pubs.acs.org.